/

Article / Book Information

Title	Turning Method that Minimizes Turning Radius for Snake-Like Robot with Active Joints and Active Wheels
Authors	Hirotaka Komura, Gen Endo, Hiroyuki Nabae, Koichi Suzumori
Citation	Proceedings of the 2016 IEEE/SICE International Symposium on System Integration, Vol. , No. , pp. 604-609
Pub. date	2016, 12
DOI	https://doi.org/10.1109/SII.2016.7844067
Copyright	(c) 2016 IEEE. Personal use of this material is permitted. Permission from IEEE must be obtained for all other users, including reprinting/republishing this material for advertising or promotional purposes, creating new collective works for resale or redistribution to servers or lists, or reuse of any copyrighted components of this work in other works.
Note	This file is author (final) version.

Turning Method that Minimizes Turning Radius for Snake-Like Robot with Active Joints and Active Wheels

Hirotaka Komura[1], Gen Endo [1], Hiroyuki Nabae [1] and Koichi Suzumori[1]

Abstract— Snake-like robot which has active joints and thruster mechanisms has been proven to have its high mobility on narrow and rough terrain because of its slim and long trunk. However, larger space than its slim trunk is necessary for snake-like robot to turn. Thus, in order to improve the mobility of snake-like robot, turning method which makes turning radius smaller is needed. In this paper, a new turning method for snake-like robot which has both pitch and yaw joints, and thruster mechanism in each module is proposed. In this method, both pitch and yaw joints are bent to their limits, and take advantage of steep bent area which are not used normally.This new method was applied to an active snake-like robot ACM-R8, and experimented in physics simulations and hardware experiments. As a result of these experiments, it was confirmed that the new method made the turning radius smaller.

I. INTRODUCTION

In general, snake-like robots have advantages in passing narrow and rough terrain and in getting over large obstacles, because of their slim and long trunks. In this point of view, snake-like robots are more suitable for exploring terrains with narrow space and large obstacles like rubble in disaster sites, than other types of transfer mechanisms such as continuous trucks or legged mechanisms.

Mechanisms of snake-like robots can be classified into three groups as shown in Table I, depending on whether their joints are active or passive, and whether each module of them has a certain thruster mechanism or not. The most general mechanisms are classified into type A which have active joints but no thruster mechanisms[1], [2]. These mechanisms generate their thrust force by serpentine motion, lateral rolling motion[3], or other specific motions. In any motions, their trunks must be bent while moving. Thus, larger space than its width are necessary for transfer.Further problems of this type is that relatively long trunk are necessary for sufficient thrust force generation.

On the other hand, type B mechanisms, which have passive joints and active thruster mechanisms in their modules, are able to move forward even if its trunk length are not enough[4]. Furthermore, trunk shape will be fit along terrain automatically because of passive joints. This phenomenon makes their thruster mechanisms to make a contact with terrain more certainly, and allows these robots to get over rough terrain. However, the transfer direction can be restricted because of passive joints which are easily bent by external force. Thus, these mechanisms can be applied to

[1]H. Komura, G Endo, H Nabae and K Suzumori are with the Department of Mechanical and Aerospace Engineering, Tokyo Institute of Technolocy, 2-12-1 Ookayama, Meguroku, Tokyo, 152-8552, Japan, komura.h.aa at m.titech.ac.jp, gendo at mes.titech.ac.jp, suzumori at mes.titech.ac.jp

TABLE I

CLASSIFICATION OF SNAKE-LIKE ROBOTS

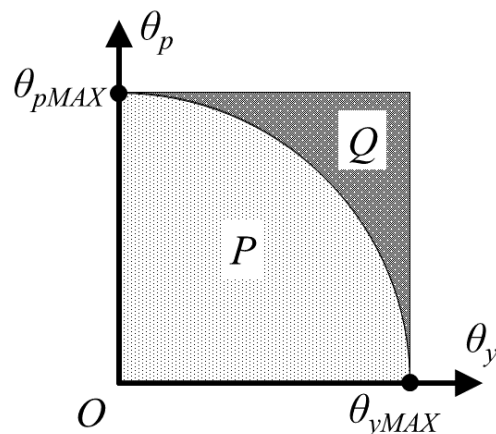|		Joint	
		Passive	Active
Thrusting	Passive		A
Mechansim	Active	B	C

Fig. 1. Photo of the ACM-R8.

Fig. 2. Graphical image of motion range of single module of snake like robot which has 2 DOFs in pitch and yaw axes. Normally, only area P is used in order to realize certain shape of trunk in any roll posture: if any joints of a snake like robot are bent to area Q, the roll posture of the robot are restricted because those joints in area Q are bent more steep than a joint which are bent in one axis at the maximum.

limited field like inspection inside pipes, and it should be difficult to use these types of robots in general purposes.

Snake-like robots with type C mechanisms, which have active joints and active thruster mechanisms are proven to have high traversability on narrow and rough terrain and large obstacles[5], [6], [7]. These types of robots also have advantages in turning radius. If we assume the trunk line of

the snake-like robot as a curve, there is a minimum arc of this trunk curve when each module is bent in one direction at the maximum. Turning radiuses of snake-like robots with type A mechanisms must be larger than the minimum arc of its trunk since this mechanism cannot generate thrust force with just an arc shape. On the other hand, type C mechanism can turn with this minimum arc, since these robots can get thrust force wich is independent of its trunk shape. Thruster mechanisms of this group are mainly wheels or continuous trucks. Continuous truck types have high mobility on rough terrain since continuous truck mechanisms have high mobility originally. However, this mechanism causes each module to be long, and makes the turning radius of snake-like robot large no matter how large motion range of each joint. On the other hand, wheel mechanisms allow the module to become shorter, and can make the turning radius smaller. For this reason, wheel mechanisms are suitable for snake-like robot which is used in narrow places.

In approximation methods for continuous curve[8], approximation accuracy between continuous curve and posture of an hardware robot is high with the joint mechanism which has pitch and yaw joints alternately in constant intervals. At the same time, such mechanisms are easy to construct, and be adopted in many cases.

Figure 2 is a graph of bending angle of single module for pitch and yaw axes. In general, only area P is used in controlling snake-like robot in order to keep trunk posture during lateral rolling. In this research, we will extend to the area Q, and propose a new method which minimizes turning radius of snake-like robot with pitch and yaw axis joints, and thruster mechanisms. Furthermore, we will apply the new method to "ACM-R8"[9](Figure 1), which we developed, and confirm the availability of the new method.

II. APPROXIMATION TO CONTINUOUS CURVE

In general, snake-like robot which is composed of large number of trunk modules possesses redundant DOFs. Thus, certain methods for deciding order values are necessary. In most cases of our researches about snake-like robots, an approximation method for continuous curve[8] is used as a control method of the robot. In the same way as our former research, an argument of this paper is also based on this continuous curve method. In this method, snake like robot is treated as a continuous curve which has no joint but is continuously bendable in every point. Figure 3 is an image of this treating.

Procedures of this method is as follows:

1) Design an appropriate continuous curve.
2) Approximate a continuous curve to a discrete model whose parameters are same as real hardware.
3) Do local control in each joint.

In this section, necessary elements of this method is explained briefly. For more detail, see [8], [9], [10].

A. Continuous Curve

In "bellows model"[10] of the continuous curve, any curves $c(s)$ can be described by only 2 shape functions,
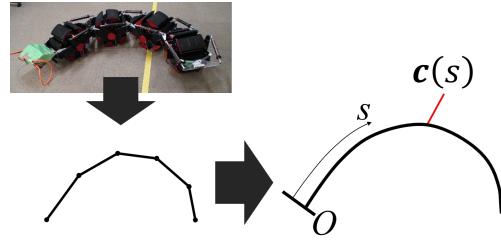

Fig. 3. Image of treating a snake-like robot as a continuous curve.

$\kappa_p(s)$ and $\kappa_y(s)$, which are defined as curvature functions in pitch or yaw directions in a positon s. Each of these functions is defined for representing windings in pitch or yaw directions. The character s is a position in the continuous curve whose length is L, and $0 \leq s \leq L$ holds if the tail tip is treated as an origin of continuous curve.

The relation equations between the continuous curve $c(s)$ and shape functions $\kappa_p(s)$, $\kappa_y(s)$ are following.

$$\begin{cases} \dfrac{dc(s)}{ds} = e_r(s) \\ \dfrac{de_r(s)}{ds} = \kappa_y(s)e_p(s) - \kappa_p(s)e_y(s) \\ \dfrac{de_p(s)}{ds} = -\kappa_y(s)e_r(s) \\ \dfrac{de_y(s)}{ds} = \kappa_p(s)e_r(s) \end{cases} \quad (1)$$

$e_r(s)$, $e_p(s)$, $e_y(s)$ are normal vectors whose directions are roll, pitch, and yaw axes of the position s of the continuous curve $c(s)$.

If both sides of Equation 1 are integrated from the origin to position s, it becomes as follows.

$$\begin{cases} c(s) = \int_0^s e_r(s)ds + c(0) \\ e_r(s) = \int_0^s (\kappa_y(s)e_p(s) - \kappa_p(s)e_y(s))ds + e_r(0) \\ e_p(s) = \int_0^s (-\kappa_y(s)e_r(s))ds + e_p(0) \\ e_y(s) = \int_0^s (\kappa_p(s)e_r(s))ds + e_y(0) \end{cases} \quad (2)$$

As this equation, the shape of the continuous curve can be decided by defining shape functions.

B. Aproximation to Discrete Curve

As the shape functions and the continuous curve are decided, approximation to the discrete model whose parameter is same as the real snake-like robot is necessary. If the snake-like robot has revolution joints in pitch and yaw axes alternately in constant intervals, an order angle of i-th joint in j-axis (j represents pitch or yaw) can be calculated by next equation, where l is a length of single module.

$$\theta_{i,j} = \int_{s_{0_{i,j}}-l/2}^{s_{0_{i,j}}+l/2} \kappa_j(s)ds \quad (3)$$

In former researches, it is major that fitting each joint position to a certain position of the continuous curve[11], [12]. On the other hand, the joint position and continuous curve don't always match up in our method. One of benefits of this method is that the simple calculation which is consisted of only integration. The low calculation cost makes calculation speed of the main controller faster, and allows us to do other calculations in some cases.

III. CONTINUOUS CURVE FOR MINIMUM TURNING

A. Regular Turning

In this turning method, all yaw axis joints are bent in the same maximum angle θ_y, as shown in the right model of Figure 5. The left model of Figure 5 are the continuous curve model of this method, and the shape function of the yaw axis $\kappa_y(s)$ becomes constant value since all joints are bent in the same angle. In this state, the relationship between the shape function and joint angle are following.

$$
\begin{aligned}
\theta_y &= \int_{-l/2}^{l/2} \kappa_y ds \\
&\Rightarrow \kappa_y = \frac{\theta_y}{l}
\end{aligned}
\tag{4}
$$

In the continuous curve approximation method, a value of the shape function of the continuous curve is same as a curvature of the curve. Thus, a radius of this curve r_y can be calculated by next equation.

$$
r_y = \frac{1}{\kappa_y} = \frac{l}{\theta_y}
\tag{5}
$$

In Figure 5, the model is constructed with 5 modules and all yaw joints are bent in $\theta_y = 36°$. Thus, the center angle of the arc of the continuous curve are $180°$.

B. Minimum Turning of the Continous Curve

While type C snake-like robots with thruster mechanisms are moving, thruster mechanisms make a contact with ground constantly, in order to generate thrust force. Thus, in most cases of motions of such robots on flat plane are done by only yaw joints.However, type C snake-like robots are also able to do motions which need both pitch and yaw joints motions like lateral rolling. Furthermore, if angles of pitch and yaw joints are independent from each other mechanically, such mechanisms can achieve steep bending in area Q in Figure 2. In this section, a new turning method, which takes an advantage of this area B, is proposed.

In the same way as Equation 4, the relationship between pitch joint angle θ_p and constant shape function κ_p becomes as follows.

$$
\kappa_p = \frac{\theta_p}{l}
\tag{6}
$$

If both pitch and yaw shape functions have certain values κ_p and κ_y, Equation 1 becomes as follows.
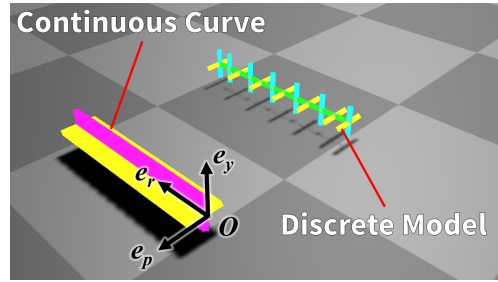

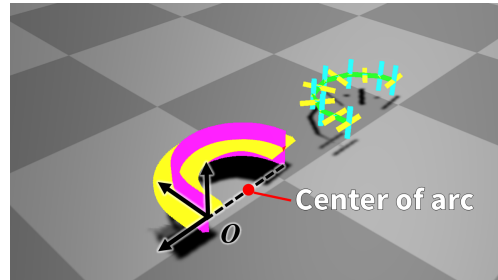Fig. 4. Image of a continuous curve and a discrete curve in straight.

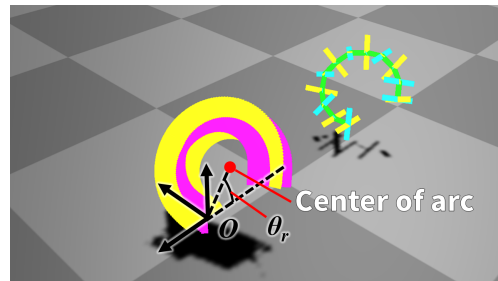Fig. 5. Image of a continuous curve and a discrete curve bent in each yaw axis.

Fig. 6. Image of a continuous curve and a discrete curve bent in yaw and pitch axes.

$$
\begin{cases}
\dfrac{d\boldsymbol{c}(s)}{ds} = \boldsymbol{e}_r(s) \\[2mm]
\dfrac{d\boldsymbol{e}_r(s)}{ds} = \kappa_y \boldsymbol{e}_p(s) - \kappa_p \boldsymbol{e}_y(s) \\[2mm]
\dfrac{d\boldsymbol{e}_p(s)}{ds} = -\kappa_y \boldsymbol{e}_r(s) \\[2mm]
\dfrac{d\boldsymbol{e}_y(s)}{ds} = \kappa_p \boldsymbol{e}_r(s)
\end{cases}
\tag{7}
$$

Equation 7 can be considered as simultaneous differential equations about $\boldsymbol{c}(s)$, which represents the position of any point of the continuous curve. Initial conditions are set as follows.

$$
\begin{cases}
\boldsymbol{c}(0) = \begin{pmatrix} 0 & 0 & 0 \end{pmatrix}^{\mathrm{T}} \\
\boldsymbol{e}_r(0) = \begin{pmatrix} 1 & 0 & 0 \end{pmatrix}^{\mathrm{T}} \\
\boldsymbol{e}_p(0) = \begin{pmatrix} 0 & 1 & 0 \end{pmatrix}^{\mathrm{T}} \\
\boldsymbol{e}_y(0) = \begin{pmatrix} 0 & 0 & 1 \end{pmatrix}^{\mathrm{T}}
\end{cases}
\tag{8}
$$

Next equation is an answer of Equation 7 about c_s, where $A = \sqrt{\kappa_p^2 + \kappa_y^2}$.

$$\begin{cases} c(s) = \begin{pmatrix} \dfrac{1}{A}\sin As \\ \dfrac{\kappa_y}{A^2}(1 - \cos As) \\ \dfrac{\kappa_p}{A^2}(1 - \cos As) \end{pmatrix} \end{cases} \tag{9}$$

Equation 9 shows that the continuous curve which are bent in yaw and pitch axes becomes a circular arc. The radius of the arc of the continuous curve becomes as follows.

$$r_{yp} = \frac{1}{A} = \frac{1}{\sqrt{\kappa_p^2 + \kappa_y^2}} = \frac{l}{\sqrt{\theta_p^2 + \theta_y^2}} \tag{10}$$

Figure 6 shows a continuous curve and a discrete model of this yaw and pitch bent model. Parameters of this model are same as the model in Figure 5. In the same way as yaw joints, the pitch joint angles are set $\kappa_p = 36°$. Following equation is a comparison between radiuses of two models in Figure 5 and Figure 6.

$$\frac{1/A}{1/\kappa_y} = \frac{\kappa_y}{\sqrt{\kappa_p^2 + \kappa_y^2}} < 1 \tag{11}$$

With this equation, the turning radius can be make smaller by bending not only yaw joints but also pitch joints.

C. Problem in Applying for an Hardware Snake-Like Robot

From Equation 11, a turning radius of a snake trunk can be $1/\sqrt{2} \fallingdotseq 0.7$ times smaller by bending not only yaw joints but also pitch joints, if the bending angles are same. In hardware environment, the plane of the arc of the continuous curve become parallel with ground, as different from the arc of continuous curve are in inclined plane in Figure 6. Thus, each module make a contact with ground in inclined posture. This is not a problem for ACM-R4.1[13] and OT-4[14] which have thrust surfaces all around their trunks, but is a problem for some snake-like robots whose thrust surfaces are not all around their trunks like ACM-R8.

Figure 7 shows a front view of a single module of ACM-R8. This module is constructed with single wide wheel and frames which exist in both side of the wheel. Thus, as the red line of the figure, this module cannot make a contact with ground and cannot generate thrust force, if it rolls more than 58°.

For this reason, the rolling angle of the proposed method must be restricted. In order to achieve the minimum turning with this restriction, yaw joints must be bent at the maximum, and pitch joints must be bent at a certain angle which fulfills this restriction.

The coordinates of center of the arc of the continuous curve are following from Equation 9.

$$\begin{pmatrix} 0 & \dfrac{\kappa_y}{A^2} & \dfrac{\kappa_p}{A^2} \end{pmatrix}^{\mathrm{T}} \tag{12}$$
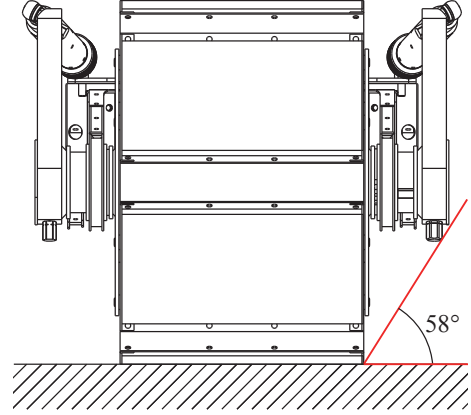
Fig. 7. One module of ACM-R8 from a back view.

TABLE II
SPEFICICATIONS OF THE ACM-R8

Length	2010 mm	Width	360 mm
Height	300 mm	Weight	36.5 kg
Number of DOFs	12	Module Interval	440 mm
Pitch Range	±90°	Yaw Range	±45°
Pitch Torque	100 Nm	Yaw Torque	100 Nm
Pitch Velocity	7.3 rpm	Yaw Velocity	7.3 rpm
Wheel Torque	32 Nm	Wheel Velocity	24.2 rpm

The roll angle can be calculated from this coordinates as follows, since the arc passes the origin O.

$$\theta_r = \arctan\frac{\kappa_y/A^2}{\kappa_p/A^2} = \arctan\frac{\kappa_y}{\kappa_p} = \arctan\frac{\theta_p}{\theta_y} \tag{13}$$

This θ_r must be smaller than the limitation angle shown in Figure 7.

IV. IMPLEMENTATION BY THE ACM-R8

A. ACM-R8

The ACM-R8(Figure 1) has 4 modules which have pitch and yaw joints, and one active wheel. Figure 8 shows the picture of single module. The feature of this robot is as follows.

- Large diameter wheel with "Swing-Grouser"[15].
- Large clearance under the body.
- Coupled driven joint mechanism for high power par weight ratio.
- Joint torque measurement system of each joint.

These features allow the robot to get over a 600 mm step and stairs, even though its height and width are only 300 mm and 360 mm.

Table II shows parameters of the ACM-R8. Pitch and yaw ranges in the table are restricted by the mechanical limitation, and the controlling limitation was defined 5° smaller than this mechanical limitation.

Fig. 8. One trunk module of the ACM-R8. Each module has 3 DOFs: One is for the wheel, and the others are for bending joint in pitch and yaw axes.
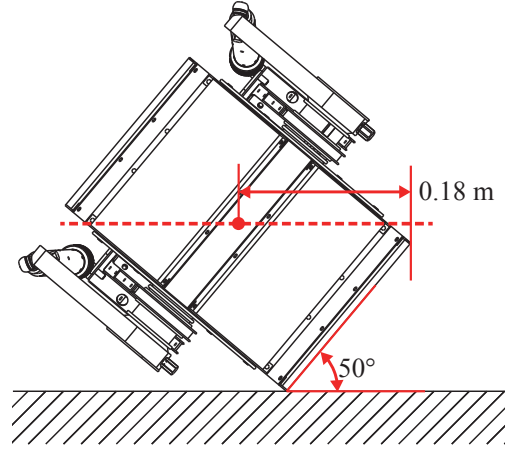

Fig. 9. Turning motion.

	Turning mehtod	Necessary width	Experimental / theoretical
Theoretical analysis	Only yaw	1.6m	100%
Theoretical analysis	Proposed method	1.2m	100%
Simulation	Only yaw	2.0m	125%
Simulation	Proposed method	1.4m	117%
Hardware experiment	Proposed method	1.3m	108%

V. APPLICATION TO THE ACM-R8

The porposed method was applied to the ACM-R8. Table III is a summary of necessary space for turning in theoretical analysis, simulation, and hardware experiment was carried out in this section.

A. Theoretical Analysis

From Table II, the maximum yaw joint angle is $40°$, and the module interval is 0.44 m. Thus, from Equation 5, r_y, the turning radius of the continuous curve of the ACM-R8 bending only yaw joint is about 0.63 m. Thus, D_y, the minimum space width for turning can be calculated as follows, since the half width of the robot w_y is 0.36 m.

$$D_y = 2 \times (r_y + w_y) \fallingdotseq 1.6[m] \tag{14}$$

The motion range of the pitch joint is quite large because of the coupled driven mechanism. However, as written in Section.V-A, there is a limitation for the rolling angle for turning. In this examination, the roll angle was set $\theta_r = 50°$, which is smaller than the limitation in Figure 7. From Equation 13, the pitch joint angle can be calculated as $\theta_p = 47.7°$. Therefore, r_{yp}, the minimum turning radius in this condition, becomes as follows.

$$r_{yp} = \frac{l}{\sqrt{\theta_p^2 + \theta_y^2}} = 0.41[m] \tag{15}$$

Additionally, $w_y p$, the half width of the module when it rolls $50°$ is also 0.18 m, as shown in Figure 9. Thus, $D_y p$, the minimum space width for turning in this situation can be calculated as follows.

$$D_{yp} = 2 \times (r_{yp} + w_{yp}) \fallingdotseq 1.2[m] \tag{16}$$

B. Simulation

A simulation experiment with a physics simulator "V-rep"[16] was done as shown in Figure 10 and Figure 11. Both pictures are top view, and images while turning are laid over in each picture. The cells in ground are $0.5m \times 0.5m$. As the physics engine, "Bullet", which was developped for games, was used and the friction coefficient in the physics engine was 1.0, and the calculation period was 10ms, and it tooks about 30s and 20s for turning with only yaw joints and turning with proposed method for each.

As a result of these simulations, the turning space width of the turning with only yaw joints was about 2.0 m, and that of the turning with proposed method was 1.4m. Although measured values were bit larger than theoretical values calculated in Section V-A, the proposed method achieved the smaller turn. The reason of errors between theoretical values and simulated values is considered that frictions between the robot and ground was not apt and lateral slippages occurred in physics simulation cases.

C. Hardware Experiment

Figure 12 shows the Hardware experiment with the ACM-R8. In this experiment, it was successful to turn with turning diameter 1.3 m including the robot width, and confirmed that the proposed method can make a smaller turn than the theoretical turning width with only yaw joints.

The reason of the errors between theoretical values and measured values are considered deviations between order values and actual joint angles, and measurement errors of the image analysis.
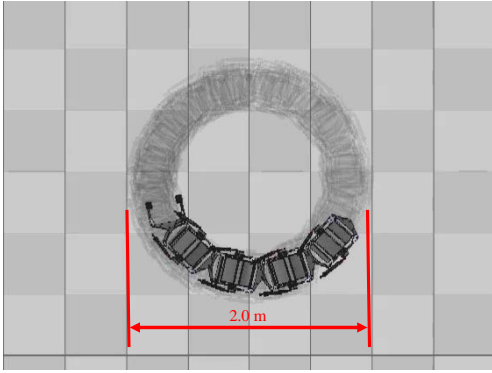
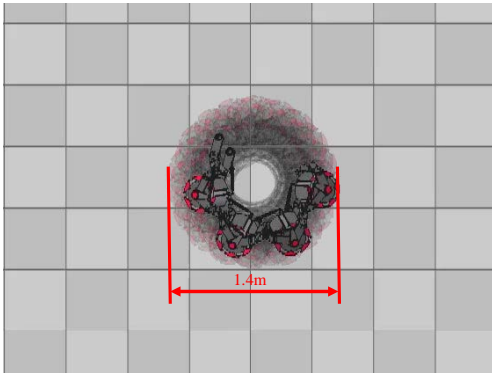Fig. 10. Turning Simulation with a Vrep simulator. Only yaw joints are bent.

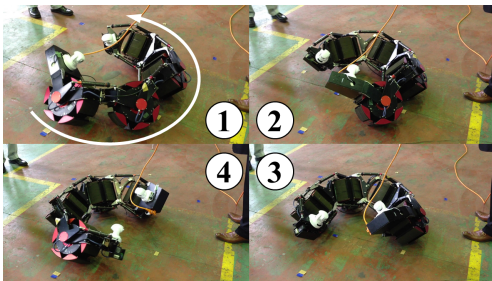Fig. 11. Turning simulation with a Vrep simulator. Both pitch and yaw joints are bent.

Fig. 12. Turning motion.

VI. CONCLUSIONS

The new turning method which take an advantage of steep bending achieve by bending both pitch and yaw joints was proposed. Furthermore, this new method was applied to the active wheeled snake-like robot "ACM-R8", and experimented in a physics simulation and a hardware experiment. As results of these experiments, it is confirmed that the proposed method can make the turning radius smaller.

As a future plan, transition method from straight posture or other any posture to proposed turning posture should be researched in order to make this method more practical.

REFERENCES

[1] H. Yamada, S. Chigisaki, M. Mori, K. Takita, K. Ogami, and S. Hirose, "Development of amphibious snake-like robot acm-r5," in *Proc.ISR2005*, 2005, p. TH3C4.

[2] C. W. III, A. M. Johnson, A. Peck, Z. McCord, A. Naaktgeboren, P. Gianfortoni, M. Gonzalez-Rivero, R. L. Hatton, and H. Choset, "Design of a modular snake robot," in *IROS*. IEEE, 2007, pp. 2609–2614.

[3] M. Mori, S. Hirose, Y. Zhang, M. Schervish, and H. Choset, "Three-dimensional serpentine motion and lateral rolling by active cord mechanism acm-r3," in *in Proc. 2002 IEEE/RSJ Int. Conf, on Intelligent Robots and Systems*, 2002, pp. 829–834.

[4] H. Kimura and S. Hirose, "Development of genbu : Active wheel passive joint articulated mobile robot," in *Intelligent Robots and Systems, 2002. IEEE/RSJ International Conference on*, vol. 1, 2002, pp. 823–828 vol.1.

[5] K. Kouno, H. Yamada, and S. Hirose, "Development of active-joint active-wheel high traversability snake-like robot acm-r4.2," *Journal of Robotics and Mechatronics*, vol. 25, no. 3, pp. 559–566, 2013.

[6] B. Klaassen and K. L. Paap, "Gmd-snake2: a snake-like robot driven by wheels and a method for motion control," in *ICRA*, 1999, pp. 3014–3019.

[7] M. Arai, Y. Tanaka, and S. Hirose, "Development of "souryu-iv" and "souryu-v:" serially connected crawler vehicles for in-rubble searching operation," *Journal of Field Robotics*, vol. 31, no. 65, 2008.

[8] H. Yamada and S. Hirose, "Study of active cord mechanism ─ approximations to continuous curves of a multi-joint body─ (in japanese)," *Journal of the robotics society of japan*, vol. 26, no. 1, pp. 110–120, 2008.

[9] H. Komura, H. Yamada, and S. Hirose, "Development of snake-like robot acm-r8 with large and mono-tread wheel," *Advanced Robotics*, 2014.

[10] H. Yamada and S. Hirose, "Study on the 3d shape of active cord mechanism," in *Proceedings 2006 IEEE International Conference on Robotics and Automation, 2006. ICRA 2006.*, May 2006, pp. 2890–2895.

[11] G. S. Chirikjian and J. W. Burdick, "A modal approach to hyper-redundant manipulator kinematics," *IEEE Transactions on Robotics and Automation*, vol. 10, no. 3, pp. 343–354, Jun 1994.

[12] S. B. Andersson, "Discrete approximations to continuous curves," in *Proceedings 2006 IEEE International Conference on Robotics and Automation, 2006. ICRA 2006.*, May 2006, pp. 2546–2551.

[13] T. Shunichi, Y. Hiroya, and H. Shigeo, "Snake-like active wheel robot acm-r4.1 with joint torque sensor and limiter." in *IROS*. IEEE, 2011, pp. 1081–1086.

[14] J. Borenstein, M. Hansen, and A. Borrell, "The omnitread ot-4 serpentine robot - design and performance." *J. Field Robotics*, vol. 24, no. 7, pp. 601–621, 2007.

[15] H. Komura, H. Yamada, S. Hirose, G. Endo, and K. Suzumori, "Study of swing-grouser wheel: A wheel for climbing high steps, even in low friction environment," in *Intelligent Robots and Systems (IROS), 2015 IEEE/RSJ International Conference on*, Sept 2015, pp. 4159–4164.

[16] E. Rohmer, S. Singh, and M. Freese, "V-rep: A versatile and scalable robot simulation framework," in *IROS 2013*, Nov 2013, pp. 1321–1326.